HHS Public Access

Author manuscript

Leukemia. Author manuscript; available in PMC 2016 May 18.

Published in final edited form as:

Leukemia. 2016 February ; 30(2): 492–500. doi:10.1038/leu.2015.247.

Chimeric antigen receptor-modified T cells derived from defined CD8+ and CD4+ subsets confer superior antitumor reactivity in vivo

Daniel Sommermeyer[*,1], **Michael Hudecek**[*,1,2], **Paula L. Kosasih**[1], **Tea Gogishvili**[2], **David G. Maloney**[1,3], **Cameron J. Turtle**[1,3], and **Stanley R. Riddell**[1,3,4]

[1]Fred Hutchinson Cancer Research Center, Clinical Research Division, Program in Immunology, Seattle, WA, United States

[2]University of Würzburg, Department of Medicine II – Hematology and Medical Oncology, Würzburg, Germany

[3]University of Washington, Department of Medicine, Seattle, WA, United States

[4]Technical University of Munich, Institute for Advanced Study, Munich, Germany

Abstract

Adoptive T-cell therapy with gene-modified T-cells expressing a tumor-reactive T-cell receptor (TCR) or chimeric antigen receptor (CAR) is a rapidly growing field of translational medicine and has shown success in the treatment of B-cell malignancies and solid tumors. In all reported trials, patients have received T-cell products comprised of random compositions of $CD4^+$ and $CD8^+$ naïve and memory T-cells, meaning that each patient received a different therapeutic agent. This variation might have influenced the efficacy of T-cell therapy, and complicates comparison of outcomes between different patients and across trials. We analyzed CD19 CAR-expressing effector T-cells derived from different subsets ($CD4^+$/$CD8^+$ naïve, central memory, effector memory). T-cells derived from each of the subsets were efficiently transduced and expanded, but showed clear differences in effector function and proliferation in vitro and in vivo. Combining the most potent $CD4^+$ and $CD8^+$ CAR-expressing subsets resulted in synergistic antitumor effects in vivo. We show that CAR-T-cell products generated from defined T-cell subsets can provide uniform potency compared with products derived from unselected T-cells that vary in phenotypic composition. These findings have important implications for the formulation of T-cell products for adoptive therapies.

To whom correspondence should be addressed: Stanley R. Riddell, MD, Fred Hutchinson Cancer Research Center, 1100 Fairview Ave N., D3-100, Seattle, 98109 WA, +1-206-667-5249, Fax: +1-206-667-7983, ; Email: sriddell@fredhutch.org

*These authors contributed equally to this work.

Conflict of interest statement:

M.H. and S.R.R. are inventors on a patent application (PCT/US1013/055862) related to this work that has been filed by the Fred Hutchinson Cancer Research Center (FHCRC) and licensed by Juno Therapeutics. S.R.R. is founder and shareholder of Juno Therapeutics.

Supplementary information is available at Leukemia's website.

Introduction

Immunotherapy with gene-modified T-cells expressing a tumor-reactive chimeric antigen receptor (CAR) is a rapidly evolving research field[1,2]. Impressive responses have been achieved in some patients with refractory acute lymphoblastic leukemia (ALL), chronic lymphocytic leukemia (CLL), and non-Hodgkin's lymphoma after infusing autologous T-cells expressing a CAR specific for the B-lineage molecule CD19[3–8]. Tumor regression appears to correlate with the level and duration of CAR-T-cell engraftment, and the subset of patients in whom CD19 CAR-T-cells proliferate and persist in the blood have continuous on-target depletion of normal $CD19^+$ B-cells and are more likely to remain in remission[3–10].

Designing optimized CARs with enhanced signaling to sustain T-cell proliferation and survival may improve the efficacy of CAR-T-cells[11–16]. Generating cell products derived from subsets of $CD8^+$ and $CD4^+$ T-cells with superior intrinsic abilities for proliferation and survival after transfer might also enhance efficacy. $CD8^+$ and $CD4^+$ T-cells exist as naïve (T_N), effector (T_E), and memory (T_M) subpopulations delineated by changes in surface phenotype after antigen exposure. T_M are further divisible into central (T_{CM}) and effector memory (T_{EM}) subsets that differ in phenotype, transcriptional profile, and self-renewal capacity[17–19]. Mouse models have defined lineage relationships of these $CD8^+$ T-cell subsets. Fate mapping of the differentiation of T_N in response to antigen supports a model in which T_N differentiate in a linear fashion to long-lived T_{CM} that serve as stem cells for antigen-specific immune responses, and to shorter-lived T_{EM} and T_E cells[18,20–22]. $CD4^+$ T-cells also express T_N, T_{CM}, and T_{EM} surface markers and provide help for cytolytic T-cells and antibody producing B-cells[23]. Clinical trials in cancer have not considered the derivation of CAR-T-cells from defined subsets despite evidence for synergy between CD8 and CD4 cells in an HIV CAR trial that might be further enhanced by subset selection[24,25]; rather $CD3^+$ T-cells are selected and non-specifically activated from PBMC with anti-CD3 mAb before transduction and expansion. This strategy simplifies manufacturing of cell products but the frequency of $CD8^+$ and $CD4^+$ T-cell subsets in the blood can differ markedly in individuals due to age, pathogen exposure, and the lymphocytotoxic effects of chemotherapy[26,27]. As a consequence, CAR-T-cell products prepared from PBMC contain divergent proportions of $CD8^+$ and $CD4^+$ T-cell subsets, and this heterogeneity could contribute to the differences in efficacy and toxicity observed in clinical trials[3,5,6,10].

Here, we purified individual $CD8^+$ and $CD4^+$ T-cell subsets from normal donors and patients with B-cell malignancies before their genetic modification with a lentiviral vector encoding a CAR, enabling analysis of the functional activity of subsets and subset combinations in vitro and in vivo. Our data show that the composition of CAR-T-cell products profoundly influences function and therapeutic efficacy, and reveals synergy between $CD4^+$ and $CD8^+$ CAR-T-cells in mediating antitumor responses in vivo.

Materials and Methods

Cells

293T cells (ATCC_CRL-11268) were cultured in DMEM/10% FCS and 100 U/ml penicillin/streptomycin and K562 (ATCC_CCL-243), K562/CD19[28], K562/ROR1[13], Raji

(ATCC_CCL-86), Raji/ffluc[29], and JeKo-1 (ATCC_CRL-3006) in RPMI-1640/5% FCS and 100 U/ml penicillin/streptomycin. Cell lines were tested monthly for the absence of mycoplasma. T-cells were cultured in RPMI-1640/10% human serum, 100 U/ml penicillin/streptomycin, 4 mM L-glutamine, 50 μM β-mercaptoethanol, and 50 U/ml IL-2. PBMC were isolated over Ficoll-Hypaque (Sigma), $CD4^+$ or $CD8^+$ T-cells were isolated by negative magnetic selection (Miltenyi), and then labeled for CD4/CD8/CD45RO/CD62L. T_N ($CD45RO^-/CD62L^+$), T_{CM} ($CD45RO^+/CD62L^+$), and T_{EM} ($CD45RO^+/CD62L^-$) were sorted to >99% purity on a FACSAriaII. PBMC from CLL patients were used as autologous CLL samples.

Vector construction, preparation of lentivirus, generation of CAR-T-cells, and in vitro functional assays

The CD19 CAR included an scFv of the CD19-specific mAb FMC63[30] with a 218 linker[31] between the VL and the VH domains, the hinge region of IgG4 with a serine to proline substitution at position 10, the CD28 transmembrane region, a 4-1BB costimulatory domain, and intracellular CD3ζ. The *CD19 CAR* gene was linked to a truncated epidermal growth factor receptor (EGFRt) by T2A and cloned into the lentiviral vector epHIV7[32]. The ROR1-specific CAR was described previously[33]. Lentivirus was generated by transient transfection of 293T cells[34] using psPAX2 and pMD2G packaging plasmids. T-cell were activated with anti-CD3/CD28-beads (Life Technologies), and transduced one day after activation by centrifugation at 800xg for 90 minutes at 32°C with lentiviral supernatant supplemented with 1 μg/mL polybrene (Millipore). T-cells were enriched for $EGFRt^+$ cells by FACS and expanded with an irradiated B-lymphoblastoid cell line (LCL)[28]. Functional in vitro assays were performed as described; cytotoxicity was analyzed by standard chromium release assays, cytokine levels by ELISA or Luminex assays; and proliferation of CAR-T-cells by carboxyfluorescein succinimidyl ester (CFSE) dilution assays[13].

Immunophenotyping

T-cells were stained with combinations of the following conjugated mAbs: CD4, CD8, CD27, CD28, CD45, CD45RA, CD45RO, CD62L, and matched isotype controls (BD Biosciences). Transduced T-cells were stained with biotin-conjugated anti-EGFR antibody (ImClone Systems Incorporated) and streptavidin-PE (BD Biosciences). Flow cytometry was performed on a FACSCantoII and data analyzed with FlowJo (Treestar).

Transfer of T-cells in NOD/SCID/$\gamma c^{-/-}$ (NSG) mice

Six to eight week old female NSG mice were obtained from the Jackson Laboratory or bred in-house, engrafted via tail vein with 5×10^5 Raji/ffluc cells, and one week later, injected i.v. with CAR- or control T-cells that had been expanded with LCL for eight or nine days. Bioluminescence imaging was performed as described[13]. Peripheral blood was obtained by retro-orbital bleeding and erythrocytes were removed using ammonium-chloride-potassium lysis buffer. At least five mice per experimental group were used for data analysis to provide 81% power to detect an effect size of 1.75, based on a t-test with a 1-sided 0.05 level of significance. The investigator was blinded to group allocation.

Statistics

A two-sided student's t-test was performed using Prism Software (GraphPad). Survival was compared by a Log-rank (Mantl-Cox) test. Results with a p-value of <0.05 were considered significant.

Study approval

Blood samples were obtained from healthy donors and from patients enrolled on a clinical trial (NCT01865617) of CD19 CAR-T-cell therapy. Normal donors and patients provided written informed consent for research protocols approved by the Institutional Review Board of the FHCRC. The FHCRC Institutional Animal Care and Use Committee approved all mouse experiments.

Results

$CD4^+$ and $CD8^+$ T-cell subsets in normal donors and patients with B-cell malignancies

We analyzed the frequency of $CD4^+$ and $CD8^+$ T-cells and the fraction of T_N ($CD45RA^+/RO^-/CD62L^+$), T_{CM} ($CD45RA^-/RO^+/CD62L^+$), and T_{EM} ($CD45RA^{+/-}/CD62L^-$) subsets in PBMC from 25 normal donors and 43 patients that were being screened for a clinical trial of CD19 CAR-T-cells. It is known that chemotherapy alters T-cell numbers and subset distribution, but variation in subsets has not been systematically analyzed for heavily pre-treated adult patients with B-cell malignancies who are candidates for CAR-T-cells. We observed substantial differences in the frequency of $CD4^+$ and $CD8^+$ T-cells between patients and normal donors, with most patients having a higher proportion of $CD8^+$ and less $CD4^+$ T-cells (Fig.1A). There was also heterogeneity in the proportions of T_N, T_{CM}, and T_{EM} subsets in individual normal donors and patients, with patient samples containing a significantly higher mean frequency of T_{EM} and lower mean frequency of T_N cells in both $CD4^+$ and $CD8^+$ subsets than normal donors (Fig.1B). These data are consistent with the large variation in the frequency of CD4 and CD8 T-cells in CAR-T-cell products reported in studies in which unselected peripheral T-cells were transduced to generate T-cells for adoptive therapy[10,35].

$CD4^+$ and $CD8^+$ CAR-T-cells are transduced efficiently and differ in effector function

Strategies for purifying T-cell subsets have been developed, making it possible to prepare products derived from defined populations[36]. To provide insight into how heterogeneity in T-cell composition might affect therapy, we evaluated functions of purified $CD4^+$ and $CD8^+$ T-cells from normal donors after transduction with a CD19-specific 4-1BB/CD3ζ CAR. The CAR vector contained the marker gene EGFRt for analysis of transduction efficiency and to enable purification of CAR-T-cells[32]. $CD4^+$ and $CD8^+$ T-cells from normal donors were transduced with similar efficiency (Fig.2A). Transgene-positive $CD4^+$ and $CD8^+$ T-cells were enriched for EGFRt expression, expanded, and effector function was analyzed. $CD8^+$ CAR-T-cells exhibited higher specific lytic activity than $CD4^+$ CAR-T-cells against $CD19^+$ Raji lymphoma and K562 cells transduced to express CD19 (K562/CD19) (Fig.2B). $CD4^+$ CAR-T-cells produced more Th1 cytokines (IFN-γ/TNF-α/IL-2) and proliferated more vigorously after tumor cell recognition compared to $CD8^+$ CAR-T-cells (Fig.2C,D). We

observed the same results with T-cells expressing a ROR1-specific CAR with a CD28 costimulatory domain demonstrating that these differences in functions of $CD4^+$ and $CD8^+$ CAR-T-cells were independent of the specificity of the CAR and the costimulatory domain in the vector (Fig.S1A–C).

Analysis of CAR function in naïve and memory $CD4^+$ T-cells

We next sort-purified $CD4^+$ T_N, T_{CM}, and T_{EM} from PBMC (Fig.3A), and transduced each subset with the CD19 CAR. Transduction of all three subsets was similar and not significantly different from unselected $CD4^+$ T-cells (Fig.S2A). CAR-T-cells at the end of in vitro culture showed uniform expression of CD45RO, including CAR-T-cells derived from the $CD45RO^-$ T_N subset, due to their activation and differentiation in culture. CD62L was retained on a higher fraction of CAR-T-cells derived from T_N and T_{CM}, CD28 expression was similar on CAR-T-cells from each subset, and CD27 was expressed by a higher fraction of CAR-T-cells derived from $CD4^+$ T_N (T_N>T_{CM}>T_{EM}) (Fig.3B). $CD4^+$ CAR-T-cells derived from T_N, T_{CM}, and T_{EM} mediated weak lytic activity against $CD19^+$ tumor cells consistent with data on unselected $CD4^+$ T-cells (Fig.3C). $CD4^+$ CAR-T-cells derived from the T_N subset produced the highest levels of cytokines after stimulation with $CD19^+$ tumor cells (Fig.3D). Greater cytokine production of CAR-T-cells from $CD4^+$ T_N cells was also observed with a ROR1-specific CD28/CD3ζ CAR (data not shown), suggesting the differences in function of CAR-T-cells derived from T_N, T_{CM}, and T_{EM} subsets reflected cell intrinsic properties.

Murine effector cells derived from less differentiated TCR-transgenic $CD8^+$ T-cell subsets are more effective in treating B16 melanoma[37], however similar data have not been shown for TCR-transgenic or CAR-modified $CD4^+$ T-cells. Thus, we analyzed the in vivo antitumor function of $CD4^+$ CAR-T-cells from each subset in NSG mice inoculated with 5×10^5 firefly-luciferase (ffluc) transduced Raji cells. Titrated doses of CAR-T-cells from T_N, T_{CM}, and T_{EM} subsets, or control EGFRt-T-cells were administered one week after tumor inoculation when mice had disseminated lymphoma. $CD4^+$ CAR-T-cells from each subset conferred a significant antitumor effect, resulting in superior survival compared with mice that received control T-cells (Fig.3E). A hierarchy in antitumor efficacy was evident by the dose titrations, with $CD4^+$ T-cells from T_N and T_{CM} conferring superior antitumor activity compared to T_{EM}-derived $CD4^+$ CAR-T-cells (Fig.3E). In vivo antitumor efficacy of the T_N- and T_{CM}-derived subsets correlated with a higher peak level of CAR-T-cells in the blood at day ten after T-cell transfer (Fig.3F). These data demonstrate that $CD4^+$ CAR-T-cells derived from T_N, T_{CM}, and T_{EM} subsets differ in cytokine production, and that $CD4^+$ T-cells from T_N and T_{CM} subsets exhibit superior antitumor activity in vivo.

Analysis of CAR function in naïve and memory $CD8^+$ T-cells

We performed a similar analysis of CAR-T-cells derived from $CD8^+$ T_N, T_{CM}, and T_{EM}. The transduction efficiencies were similar in all three subsets and not significantly different from unselected $CD8^+$ T-cells (Fig.S2B). Phenotypic analysis of the $CD8^+$ CAR-T-cells from each subset showed uniform expression of CD45RO, and higher levels of CD62L on CAR-T-cells from $CD8^+$ T_N and T_{CM} compared with T_{EM} (Fig.4A). CAR-T-cells derived from $CD8^+$ T_N, T_{CM}, and T_{EM} mediated near-equivalent specific lysis of $CD19^+$ tumor cells (Fig.4B), and

T_N-derived CAR-T-cells produced more cytokines than T_{CM}- and T_{EM}-derived CAR-T-cells in response to stimulation with $CD19^+$ tumor cells (Fig.4C). Notably, the amount of IL-2 produced by all CAR-T-cells derived from $CD8^+$ T-cell subsets (mean IL-2 concentration (pg/ml) after stimulation with Raji; T_N: 716, T_{CM}: 36, T_{EM} 30) was substantially less than by CAR-T-cells derived from the corresponding $CD4^+$ T-cells (T_N: 2798, T_{CM}: 369, T_{EM} 315).

We analyzed the antitumor function of $CD8^+$ CAR-T-cells from each subset at two dose levels in the NSG/Raji/ffluc model. At the lower dose (1×10^6), $CD8^+$ CAR-T-cells from T_{CM} conferred the longest survival, whereas $CD8^+$ CAR-T_N and T_{EM} were less effective (Fig.4D). This hierarchy was confirmed at the higher dose (2.5×10^6) where all mice treated with T_{CM}-derived CAR-T-cells survived tumor-free. The superior efficacy of $CD8^+$ CAR-T-cells derived from T_{CM} was associated with greater proliferation in vivo (Fig.4E), consistent with our previous observations and other pre-clinical models[38,39]. Thus, similar to $CD4^+$ T-cells, CD19 CAR-T-cells from $CD8^+$ T_N, T_{CM}, and T_{EM} exhibit differences in effector functions in vitro and antitumor efficacy in vivo. It is noteworthy that the peak frequency of CAR-T-cells derived from all $CD4^+$ T-cell subsets, including $CD4^+$ T_{EM} that was incapable of eradicating tumor in a majority of mice, exceeded that of a curative dose of $CD8^+$ T_{CM}-derived CAR-T-cells, illustrating the greater potency of $CD8^+$ CAR-T-cells derived from this subset (Fig.3F,4E; and data not shown).

$CD4^+$ CAR-T-cells exhibit synergistic antitumor activity with $CD8^+$ CAR-T-cells

In addition to direct tumor recognition, the production of abundant IL-2 by $CD4^+$ CAR-T-cells might augment proliferation, survival, and efficacy of $CD8^+$ CAR-T-cells. Synergistic activity of CD4 and CD8 CAR-T-cells has been observed in murine models[40,41], although derivation from memory and naïve subsets was not studied. Thus, we examined potential synergy between adoptively transferred $CD4^+$ CAR-T-cells and $CD8^+$ CAR-T-cells derived from T_{CM}, which was the most efficacious CD8 subset alone. We first evaluated whether $CD4^+$ CD19 CAR-T-cells derived from T_N, T_{CM}, and T_{EM} subsets augmented in vitro proliferation of $CD8^+$ T_{CM}-derived CAR-T-cells because peak numbers of CAR-T-cells in vivo correlated with antitumor efficacy in our tumor model, and has been an important parameter in clinical trials. We determined proliferation of $CD8^+$ T_{CM}-derived CAR-T-cells alone and combined with $CD4^+$ CAR-T-cells by CFSE dye dilution after stimulation with $CD19^+$ tumor cells. $CD4^+$ CAR-T-cells derived from T_N, T_{CM}, and T_{EM} subsets of normal donors enhanced the proliferation of $CD8^+$ T_{CM}-derived CAR-T-cells in response to stimulation with $CD19^+$ JeKo-1 cells, with $CD4^+$ T_N providing the greatest enhancement (Fig.5A). Even after stimulation with $CD80^+/CD86^+$ Raji cells, the proliferation of $CD8^+$ T_{CM}-derived CAR-T-cells was increased by the addition of $CD4^+$ CAR-T-cells derived from the T_N subset.

Because $CD4^+$ T-cells from patients with B-cell malignancies may be functionally compromised[42,43], we analyzed whether helper function was preserved in $CD4^+$ CAR-T-cells generated from $CD4^+$ T_N, T_{CM}, and T_{EM} subsets of CLL patients. The cytokine profile of patient $CD4^+$ CAR-T-cells was similar to that observed in normal donors ($T_N > T_{CM}/T_{EM}$) suggesting that transduction and culture of T-cells from these patients may overcome any

functional defects, or result in the selective expansion of T-cells that were competent to produce cytokines (Fig.5B). As observed with normal donors, the proliferation of $CD8^+$ T_{CM}-derived CAR-T-cells from patients after stimulation with a tumor cell line and with the patient's primary autologous leukemia cells was augmented when autologous $CD4^+$ CAR-T-cells were included in the co-culture, and $CD4^+$ CAR-T-cells from the T_N subset provided the greatest enhancement of $CD8^+$ T_{CM}-derived CAR-T-cell proliferation (Fig.5C).

To determine whether a synergistic antitumor effect of $CD8^+$ and $CD4^+$ CAR-T-cells was evident in vivo, NSG mice with Raji tumors were treated with an effective but non-curative dose (8×10^5) of either $CD8^+$ or $CD4^+$ CD19 CAR-T-cells derived from the T_{CM} subsets, or with the same total dose of CAR-T-cells but consisting of a 1:1 ratio of $CD8^+$ T_{CM}-derived and $CD4^+$ CAR-T-cells derived from each of the T_N, T_{CM}, or T_{EM} subsets. The data show that the combination of $CD8^+$ T_{CM}-derived CAR-T-cells with $CD4^+$ CAR-T-cells from either the T_N or T_{CM} subsets conferred superior antitumor activity compared to CAR-T-cells derived from either $CD8^+$ or $CD4^+$ T_{CM} subsets alone, or the $CD8^+$ T_{CM}/$CD4^+$ T_{EM} combination (Fig.5D,E). Analysis of the frequency of CAR-T-cells in the peripheral blood of mice showed that the improved antitumor effect in mice receiving CAR-T-cells derived from $CD8^+$ T_{CM} combined with $CD4^+$ T_{CM} or T_N correlated with greater peak proliferation of $CD8^+$ T-cells in vivo than observed with the $CD8^+$ T_{CM} product alone or with $CD4^+$ T_{EM}, consistent with the hierarchy observed in the in vitro experiments (Fig.5F,G). We also observed significant in vivo expansion of $CD4^+$ CAR-T-cells when administered alone, however at this cell dose $CD4^+$ CAR-T-cells were insufficient to prevent outgrowth of Raji tumors, despite sustained proliferation and persistence for more than four weeks (Fig.5F).

In healthy donors, T_N and T_{CM} are the numerically dominant $CD4^+$ T-cell subsets (Fig.1), and we found that CAR-T-cells derived from unselected bulk $CD4^+$ were equivalently effective in providing help as sort purified $CD4^+$ T_N and $CD4^+$ T_{CM}, although the enhancement of $CD8^+$ CAR-T-cell proliferation with unselected $CD4^+$ T-cells was less than that observed with $CD4^+$ T_N or $CD4^+$ T_{CM}-derived products (data not shown). Our data on the subset distribution in patients with B-cell malignancies eligible for CD19 CAR-T-cell therapy shows a marked increase in the proportion of $CD4^+$ T_{EM}, suggesting that improvements in potency in some patients may be achieved by selecting $CD4^+$ T_N and T_{CM} subsets prior to preparing therapeutic products.

Patient CAR-T-cell products of defined subset composition have enhanced potency in vivo

To evaluate the potential advantages of preparing cell products of defined subset composition in a clinical setting, we prepared CD19 CAR-T-cells from two patients with non-Hodgkin's lymphoma enrolled on an ongoing clinical trial of CAR-T-cell therapy (NCT01865617), and used these cell products to treat NSG mice engrafted with Raji/ffluc. We derived CD19 CAR-T-cells from unselected PBMC, or defined populations of sort-purified $CD62L^+$/$CD45RO^+$ CD8 T_{CM}, $CD62L^+$/$CD45RO^-$ CD4 T_N and unselected CD4 T-cells (CD4 T_{US}) (Fig.6A). From each starting population, CD19 CAR-T-cells expanded at similar rates and to clinically useful therapeutic numbers. Phenotype analysis showed that the CAR-T-cells derived from whole PBMC was further skewed after transduction and

contained mainly $CD8^+$ T-cells and a smaller proportion of $CD4^+$ CAR-T-cells (approx. 6:1 ratio) (Fig.6B).

NSG mice with Raji tumors were then treated with a fixed total dose of 1×10^6 CAR-T-cells derived from either PBMC, $CD8^+$ T_{CM}, $CD4^+$ T_N, or a combined product of $CD8^+$ T_{CM} and $CD4^+$ T-cells (T_N or T_{US}) at a 1:1 ratio. Analysis of tumor progression and survival showed enhanced antitumor efficacy of cell products comprised of $CD8^+$ T_{CM} and either $CD4^+$ T_N or T_{US} compared to products from PBMC, or from $CD8^+$ or $CD4^+$ T-cells alone (Fig.6C,D). The combination of $CD8^+$ T_{CM} and $CD4^+$ T_N conferred the strongest antitumor effect, and long-term tumor-free survival was achieved in all mice in this treatment group (n=5/5). Complete tumor eradication was also observed in a subset of the mice that received the combination of $CD8^+$ T_{CM} and $CD4^+$ T_{US} (n=1/5). All mice in the group that received PBMC-derived CAR-T-cells expired from progressive tumors. We again found a strong correlation between enhanced antitumor efficacy and superior proliferation of $CD8^+$ CAR-T-cells (Fig.6E). The data show that formulating $CD8^+$ and $CD4^+$ CAR-T-cells from defined progeny can provide cell products with increased potency compared with CAR-T-cells from whole unselected PBMC or the $CD8^+$ T-cell subset alone.

Discussion

Clinical trials in which peripheral blood T-cells were transduced with CD19 CARs containing CD28/CD3ζ or 4-1BB/CD3ζ signaling domains demonstrate a high complete remission rate in ALL and a significant response rate in CLL and non-Hodgkin's lymphoma[3–10,35,44]. Not all patients respond and toxicities, including cytokine release syndrome, disseminated intravascular coagulopathy, and neurotoxicity can occur after infusing CAR-T-cells[3,6]. The follow-up in most trials is short, and the durability of responses remains to be determined. Comparing efficacy and toxicity outcomes in different studies is difficult because of patient heterogeneity and differences in vector design, culture methods, and cell doses[3–10,35,44]. Furthermore, our data show that the frequencies of $CD4^+$ and $CD8^+$ T-cells, and the proportions of naïve and memory cells in each subset, are skewed in patients with B-cell malignancies that have received cytotoxic chemotherapy. Thus, in the absence of selection of defined populations, the phenotype and function of genetically modified cell products prepared from patients will be diverse and reflective of the proportions of $CD4^+$ and $CD8^+$ T-cells and memory and naïve subsets in the blood. Indeed, clinical trials of CD19 CAR-T-cells have administered products that diverge markedly in the proportions of $CD4^+$ and $CD8^+$ T-cells, and it is impossible to retrospectively determine the fraction of transduced T-cells that were derived from naïve or memory T-cell precursors[3,35].

The efficacy of T-cell therapy is predicated on the ability of transferred cells to proliferate in vivo to overcome numerically larger tumor burdens, migrate to tumor sites, persist, and mediate effector functions that destroy tumor cells. Independent of subset derivation, in vitro activated T-cells acquire cytotoxicity and cytokine production. However, prior studies in mice and non-human primates have shown that the persistence and function of adoptively transferred effector $CD8^+$ T-cells differs depending on the T-cell subsets from which they were derived. The transfer of cytomegalovirus-specific $CD8^+$ T-cell clones derived from T_{CM} but not T_{EM} provided persistent immunity for more than four years[38,45]; and TCR-

transgenic T-cells derived from the T_N and T_{CM} subsets conferred superior antitumor responses to melanoma than those derived from T_{EM}[37,46]. Pharmacologic activation of Wnt signaling during the culture of $CD8^+$ T_N arrests differentiation at a phenotype intermediate between T_N and T_{CM}, and these arbitrarily termed “memory stem cells” have potent antitumor activity in animals[47]. Human T-cells with this phenotype are present in blood as a minor population and when engineered with CARs and administered with $CD4^+$ T-cells are effective in tumor xenograft models[19]. However, strategies for purification of this subset for clinical use are not available.

Unlike oncology drugs where dose/response relationships are readily measurable, CAR-T-cells prepared from unselected cell populations might vary widely in potency. To provide insight into how variation in common subsets might affect therapy with CAR-T-cells, we transduced individual $CD8^+$ and $CD4^+$ T-cell subsets from normal donors and patients with B-cell malignancies with a CD19 CAR. All $CD4^+$ and $CD8^+$ T-cell subsets mediated cytolysis, secreted cytokines, and proliferated in response to tumor cells in vitro. Unselected $CD4^+$ CAR-T-cells and those derived from T_N, T_{CM}, and T_{EM} subsets were less cytolytic and produced higher levels of cytokines than unselected $CD8^+$ CAR-T-cells. CAR-T-cells derived from $CD4^+$ T_N produced more cytokines than those derived from $CD4^+$ T_{CM} and T_{EM}, and a similar hierarchy of cytokine production was evident in CAR-T-cells derived from $CD8^+$ T-cells. These differences in functional properties were evident with T-cells from normal donors and from patients with B-cell malignancies, demonstrating that although phenotypic composition was skewed in patients, subset intrinsic functional properties were retained when the T cells were signaled through the CAR.

Differences in antitumor efficacy depending on the phenotype and subset derivation of CAR-T-cells were demonstrated by experiments in NSG mice engrafted with $CD19^+$ Raji tumors. The efficacy of $CD4^+$ CAR-T-cells derived from different subsets has not previously been examined. Our data show that $CD4^+$ CAR-T-cells derived from T_N and T_{CM} were more effective than those from T_{EM}, which is the subset that is most increased in frequency in patients. $CD8^+$ CAR-T-cells derived from T_{CM} and T_N were also more effective than those derived from $CD8^+$ T_{EM}. There was a correlation between antitumor activity and peak proliferation of $CD4^+$ and $CD8^+$ CAR-T-cells, consistent with observations in patients.

A notable finding in our studies of human CD19 CAR-T-cell products that extends prior work in mice with bulk CD4/CD8 T cell subsets[40,41] was that the potency was dramatically enhanced by formulating $CD8^+$ CAR-T-cells derived from T_{CM} with $CD4^+$ CAR-T-cells, and especially with $CD4^+$ CAR-T-cells derived from T_N. Formulating cell products in a 1:1 CD4/CD8 ratio resulted in complete eradication of Raji lymphoma at cell doses that were ineffective with either subset alone. Efficacy correlated with markedly greater proliferation of $CD8^+$ CAR-T-cells, suggesting that IL-2 produced by $CD4^+$ T-cells (T_N>T_{CM}>T_{EM}) was important in sustaining the $CD8^+$ T-cell response. The relevance of these findings to clinical applications was demonstrated by the enhanced potency of CD19 CAR-T-cells prepared from defined T-cell subsets compared with unselected PBMC obtained from patients with B-cell lymphoma. Based on the compelling results in the preclinical experiments reported here, we have initiated a clinical trial of CD19 CAR-T-cells of defined subset composition (https://clinicaltrials.gov/ct2/show/NCT01865617).

CAR-T-cells represent a new and promising approach to cancer therapy, however heterogeneity of cell products used in different clinical trials makes it difficult to interpret the basis for therapeutic success or failure. Adoptive therapy with defined cell products will require GMP compliant cell selection methods that do not leave bound reagents on the T-cells. Advances in cell selection methodologies have recently been made[36], and it is likely that automated devices will be developed to improve producing T-cell products of defined composition. Identifying the most effective compositions of CAR-T-cells will require evaluation in carefully designed clinical trials and may be most critical in solid tumors where target molecules are expressed at lower densities than CD19, and immunosuppressive tumor microenvironments pose an obstacle to tumor eradication. Our results suggest that defining the composition of T-cells used in adoptive therapy can enhance antitumor activity, lower the T-cell doses needed for therapeutic efficacy, and reduce a major variable that currently complicates comparison of results in individual patients and across studies.

Supplementary Material

Refer to Web version on PubMed Central for supplementary material.

Acknowledgments

The authors would like to thank Melissa Comstock (Shared Resources, FHCRC) for expertise in performing the mouse experiments. This work was supported by grants from the National Institutes of Health CA136551, CA18029, and CA114536 (S.R.R.). D.S. and M.H. were supported by the German Research Foundation (DFG, Deutsche Forschungsgemeinschaft, SO1214/1-1, HU1668/1-1, 1-2,). M.H. was supported by the Leukemia and Lymphoma Society (LLS, 5520-11), the German Cancer Aid (Deutsche Krebshilfe e.V., Max Eder Program 110313), and the University of Würzburg (Interdisziplinäres Zentrum für Klinische Forschung, IZKF, Z-4/109 and D-244).

References

1. Jensen MC, Riddell SR. Design and implementation of adoptive therapy with chimeric antigen receptor-modified T cells. Immunol Rev. 2014 Jan; 257(1):127–144. [PubMed: 24329794]
2. Kochenderfer JN, Rosenberg SA. Treating B-cell cancer with T cells expressing anti-CD19 chimeric antigen receptors. Nature reviews Clinical oncology. 2013 May; 10(5):267–276.
3. Davila ML, Riviere I, Wang X, Bartido S, Park J, Curran K, et al. Efficacy and Toxicity Management of 19-28z CAR T Cell Therapy in B Cell Acute Lymphoblastic Leukemia. Sci Transl Med. 2014 Feb 19.6(224):224ra225.
4. Grupp SA, Kalos M, Barrett D, Aplenc R, Porter DL, Rheingold SR, et al. Chimeric antigen receptor-modified T cells for acute lymphoid leukemia. N Engl J Med. 2013 Apr 18; 368(16):1509–1518. [PubMed: 23527958]
5. Kalos M, Levine BL, Porter DL, Katz S, Grupp SA, Bagg A, et al. T cells with chimeric antigen receptors have potent antitumor effects and can establish memory in patients with advanced leukemia. Sci Transl Med. 2011 Aug 10.3(95):95ra73.
6. Kochenderfer JN, Dudley ME, Feldman SA, Wilson WH, Spaner DE, Maric I, et al. B-cell depletion and remissions of malignancy along with cytokine-associated toxicity in a clinical trial of anti-CD19 chimeric-antigen-receptor-transduced T cells. Blood. 2012 Mar 22; 119(12):2709–2720. [PubMed: 22160384]
7. Porter DL, Levine BL, Kalos M, Bagg A, June CH. Chimeric antigen receptor-modified T cells in chronic lymphoid leukemia. N Engl J Med. 2011 Aug 25; 365(8):725–733. [PubMed: 21830940]
8. Maude SL, Frey N, Shaw PA, Aplenc R, Barrett DM, Bunin NJ, et al. Chimeric antigen receptor T cells for sustained remissions in leukemia. N Engl J Med. 2014 Oct 16; 371(16):1507–1517. [PubMed: 25317870]

9. Savoldo B, Ramos CA, Liu E, Mims MP, Keating MJ, Carrum G, et al. CD28 costimulation improves expansion and persistence of chimeric antigen receptor-modified T cells in lymphoma patients. The Journal of clinical investigation. 2011 May; 121(5):1822–1826. [PubMed: 21540550]
10. Brentjens RJ, Riviere I, Park JH, Davila ML, Wang X, Stefanski J, et al. Safety and persistence of adoptively transferred autologous CD19-targeted T cells in patients with relapsed or chemotherapy refractory B-cell leukemias. Blood. 2011 Nov 3; 118(18):4817–4828. [PubMed: 21849486]
11. Brentjens RJ, Santos E, Nikhamin Y, Yeh R, Matsushita M, La Perle K, et al. Genetically targeted T cells eradicate systemic acute lymphoblastic leukemia xenografts. Clin Cancer Res. 2007 Sep 15; 13(18 Pt 1):5426–5435. [PubMed: 17855649]
12. Carpenito C, Milone MC, Hassan R, Simonet JC, Lakhal M, Suhoski MM, et al. Control of large, established tumor xenografts with genetically retargeted human T cells containing CD28 and CD137 domains. Proc Natl Acad Sci U S A. 2009 Mar 3; 106(9):3360–3365. [PubMed: 19211796]
13. Hudecek M, Lupo-Stanghellini MT, Kosasih PL, Sommermeyer D, Jensen MC, Rader C, et al. Receptor Affinity and Extracellular Domain Modifications Affect Tumor Recognition by ROR1-Specific Chimeric Antigen Receptor T Cells. Clin Cancer Res. 2013 Jun 15; 19(12):3153–3164. [PubMed: 23620405]
14. James SE, Greenberg PD, Jensen MC, Lin Y, Wang J, Till BG, et al. Antigen sensitivity of CD22-specific chimeric TCR is modulated by target epitope distance from the cell membrane. J Immunol. 2008 May 15; 180(10):7028–7038. [PubMed: 18453625]
15. Kowolik CM, Topp MS, Gonzalez S, Pfeiffer T, Olivares S, Gonzalez N, et al. CD28 costimulation provided through a CD19-specific chimeric antigen receptor enhances in vivo persistence and antitumor efficacy of adoptively transferred T cells. Cancer Res. 2006 Nov 15; 66(22):10995–11004. [PubMed: 17108138]
16. Milone MC, Fish JD, Carpenito C, Carroll RG, Binder GK, Teachey D, et al. Chimeric receptors containing CD137 signal transduction domains mediate enhanced survival of T cells and increased antileukemic efficacy in vivo. Molecular therapy: the journal of the American Society of Gene Therapy. 2009 Aug; 17(8):1453–1464. [PubMed: 19384291]
17. Kaech SM, Hemby S, Kersh E, Ahmed R. Molecular and functional profiling of memory CD8 T cell differentiation. Cell. 2002 Dec 13; 111(6):837–851. [PubMed: 12526810]
18. Graef P, Buchholz VR, Stemberger C, Flossdorf M, Henkel L, Schiemann M, et al. Serial transfer of single-cell-derived immunocompetence reveals stemness of CD8(+) central memory T cells. Immunity. 2014 Jul 17; 41(1):116–126. [PubMed: 25035956]
19. Gattinoni L, Lugli E, Ji Y, Pos Z, Paulos CM, Quigley MF, et al. A human memory T cell subset with stem cell-like properties. Nat Med. 2011 Oct; 17(10):1290–1297. [PubMed: 21926977]
20. Stemberger C, Huster KM, Koffler M, Anderl F, Schiemann M, Wagner H, et al. A single naive CD8+ T cell precursor can develop into diverse effector and memory subsets. Immunity. 2007 Dec; 27(6):985–997. [PubMed: 18082432]
21. Buchholz VR, Flossdorf M, Hensel I, Kretschmer L, Weissbrich B, Graf P, et al. Disparate individual fates compose robust CD8+ T cell immunity. Science. 2013 May 3; 340(6132):630–635. [PubMed: 23493420]
22. Gerlach C, Rohr JC, Perie L, van Rooij N, van Heijst JW, Velds A, et al. Heterogeneous differentiation patterns of individual CD8+ T cells. Science. 2013 May 3; 340(6132):635–639. [PubMed: 23493421]
23. Rocha B, Tanchot C. Towards a cellular definition of CD8+ T-cell memory: the role of CD4+ T-cell help in CD8+ T-cell responses. Current opinion in immunology. 2004 Jun; 16(3):259–263. [PubMed: 15134772]
24. Mitsuyasu RT, Anton PA, Deeks SG, Scadden DT, Connick E, Downs MT, et al. Prolonged survival and tissue trafficking following adoptive transfer of CD4zeta gene-modified autologous CD4(+) and CD8(+) T cells in human immunodeficiency virus-infected subjects. Blood. 2000 Aug 1; 96(3):785–793. [PubMed: 10910888]
25. Walker RE, Bechtel CM, Natarajan V, Baseler M, Hege KM, Metcalf JA, et al. Long-term in vivo survival of receptor-modified syngeneic T cells in patients with human immunodeficiency virus infection. Blood. 2000 Jul 15; 96(2):467–474. [PubMed: 10887107]

26. Mackall CL, Fleisher TA, Brown MR, Andrich MP, Chen CC, Feuerstein IM, et al. Age, thymopoiesis, and CD4+ T-lymphocyte regeneration after intensive chemotherapy. N Engl J Med. 1995 Jan 19; 332(3):143–149. [PubMed: 7800006]
27. Hakim FT, Cepeda R, Kaimei S, Mackall CL, McAtee N, Zujewski J, et al. Constraints on CD4 recovery postchemotherapy in adults: thymic insufficiency and apoptotic decline of expanded peripheral CD4 cells. Blood. 1997 Nov 1; 90(9):3789–3798. [PubMed: 9345067]
28. Terakura S, Yamamoto TN, Gardner RA, Turtle CJ, Jensen MC, Riddell SR. Generation of CD19-chimeric antigen receptor modified CD8+ T cells derived from virus-specific central memory T cells. Blood. 2012 Jan 5; 119(1):72–82. [PubMed: 22031866]
29. Hudecek M, Sommermeyer D, Kosasih PL, Silva-Benedict A, Liu L, Rader C, et al. The nonsignaling extracellular spacer domain of chimeric antigen receptors is decisive for in vivo antitumor activity. Cancer immunology research. 2015 Feb; 3(2):125–135. [PubMed: 25212991]
30. Zola H, MacArdle PJ, Bradford T, Weedon H, Yasui H, Kurosawa Y. Preparation and characterization of a chimeric CD19 monoclonal antibody. Immunology and cell biology. 1991 Dec.69:411–422. [PubMed: 1725979]
31. Whitlow M, Bell BA, Feng SL, Filpula D, Hardman KD, Hubert SL, et al. An improved linker for single-chain Fv with reduced aggregation and enhanced proteolytic stability. Protein engineering. 1993 Nov; 6(8):989–995. [PubMed: 8309948]
32. Wang X, Chang WC, Wong CW, Colcher D, Sherman M, Ostberg JR, et al. A transgene-encoded cell surface polypeptide for selection, in vivo tracking, and ablation of engineered cells. Blood. 2011 Aug 4; 118(5):1255–1263. [PubMed: 21653320]
33. Hudecek M, Schmitt TM, Baskar S, Lupo-Stanghellini MT, Nishida T, Yamamoto TN, et al. The B-cell tumor-associated antigen ROR1 can be targeted with T cells modified to express a ROR1-specific chimeric antigen receptor. Blood. 2010 Nov 25; 116(22):4532–4541. [PubMed: 20702778]
34. Leisegang M, Engels B, Meyerhuber P, Kieback E, Sommermeyer D, Xue SA, et al. Enhanced functionality of T cell receptor-redirected T cells is defined by the transgene cassette. J Mol Med. 2008 May; 86(5):573–583. [PubMed: 18335188]
35. Lee DW, Kochenderfer JN, Stetler-Stevenson M, Cui YK, Delbrook C, Feldman SA, et al. T cells expressing CD19 chimeric antigen receptors for acute lymphoblastic leukaemia in children and young adults: a phase 1 dose-escalation trial. Lancet. 2015 Feb 7; 385(9967):517–528. [PubMed: 25319501]
36. Stemberger C, Dreher S, Tschulik C, Piossek C, Bet J, Yamamoto TN, et al. Novel serial positive enrichment technology enables clinical multiparameter cell sorting. PloS one. 2012; 7(4):e35798. [PubMed: 22545138]
37. Hinrichs CS, Borman ZA, Cassard L, Gattinoni L, Spolski R, Yu Z, et al. Adoptively transferred effector cells derived from naive rather than central memory CD8+ T cells mediate superior antitumor immunity. Proc Natl Acad Sci U S A. 2009 Oct 13; 106(41):17469–17474. [PubMed: 19805141]
38. Berger C, Jensen MC, Lansdorp PM, Gough M, Elliott C, Riddell SR. Adoptive transfer of effector CD8+ T cells derived from central memory cells establishes persistent T cell memory in primates. The Journal of clinical investigation. 2008 Jan; 118(1):294–305. [PubMed: 18060041]
39. Wang X, Berger C, Wong CW, Forman SJ, Riddell SR, Jensen MC. Engraftment of human central memory-derived effector CD8+ T cells in immunodeficient mice. Blood. 2011 Feb 10; 117(6): 1888–1898. [PubMed: 21123821]
40. Moeller M, Haynes NM, Kershaw MH, Jackson JT, Teng MW, Street SE, et al. Adoptive transfer of gene-engineered CD4+ helper T cells induces potent primary and secondary tumor rejection. Blood. 2005 Nov 1; 106(9):2995–3003. [PubMed: 16030195]
41. Moeller M, Kershaw MH, Cameron R, Westwood JA, Trapani JA, Smyth MJ, et al. Sustained antigen-specific antitumor recall response mediated by gene-modified CD4+ T helper-1 and CD8+ T cells. Cancer Res. 2007 Dec 1; 67(23):11428–11437. [PubMed: 18056471]
42. Riches JC, Davies JK, McClanahan F, Fatah R, Iqbal S, Agrawal S, et al. T cells from CLL patients exhibit features of T-cell exhaustion but retain capacity for cytokine production. Blood. 2013 Feb 28; 121(9):1612–1621. [PubMed: 23247726]

43. Kiaii S, Clear AJ, Ramsay AG, Davies D, Sangaralingam A, Lee A, et al. Follicular lymphoma cells induce changes in T-cell gene expression and function: potential impact on survival and risk of transformation. Journal of clinical oncology: official journal of the American Society of Clinical Oncology. 2013 Jul 20; 31(21):2654–2661. [PubMed: 23775959]

44. Kochenderfer JN, Dudley ME, Kassim SH, Somerville RP, Carpenter RO, Stetler-Stevenson M, et al. Chemotherapy-Refractory Diffuse Large B-Cell Lymphoma and Indolent B-Cell Malignancies Can Be Effectively Treated With Autologous T Cells Expressing an Anti-CD19 Chimeric Antigen Receptor. Journal of clinical oncology: official journal of the American Society of Clinical Oncology. 2015 Feb 20; 33(6):540–549. [PubMed: 25154820]

45. Berger C, Berger M, Anderson D, Riddell SR. A non-human primate model for analysis of safety, persistence, and function of adoptively transferred T cells. Journal of medical primatology. 2011 Apr; 40(2):88–103. [PubMed: 21044089]

46. Klebanoff CA, Gattinoni L, Torabi-Parizi P, Kerstann K, Cardones AR, Finkelstein SE, et al. Central memory self/tumor-reactive CD8+ T cells confer superior antitumor immunity compared with effector memory T cells. Proc Natl Acad Sci U S A. 2005 Jul 5; 102(27):9571–9576. [PubMed: 15980149]

47. Gattinoni L, Zhong XS, Palmer DC, Ji Y, Hinrichs CS, Yu Z, et al. Wnt signaling arrests effector T cell differentiation and generates CD8+ memory stem cells. Nat Med. 2009 Jul; 15(7):808–813. [PubMed: 19525962]

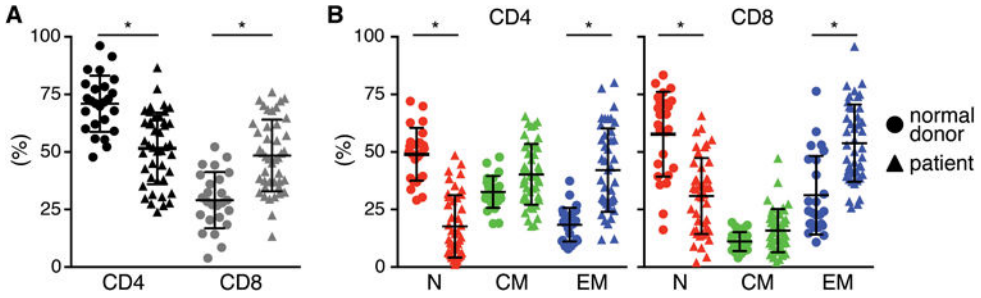

Figure 1. T-cell subset composition in PBMC from patients and healthy donors

Proportions of **(A)** $CD4^+$ and $CD8^+$ T-cells, and **(B)** T_N, T_{CM}, and T_{EM} cell subsets in blood of patients with B-cell malignancies and normal donors. Asterisk indicates significant differences between normal donors and patients.

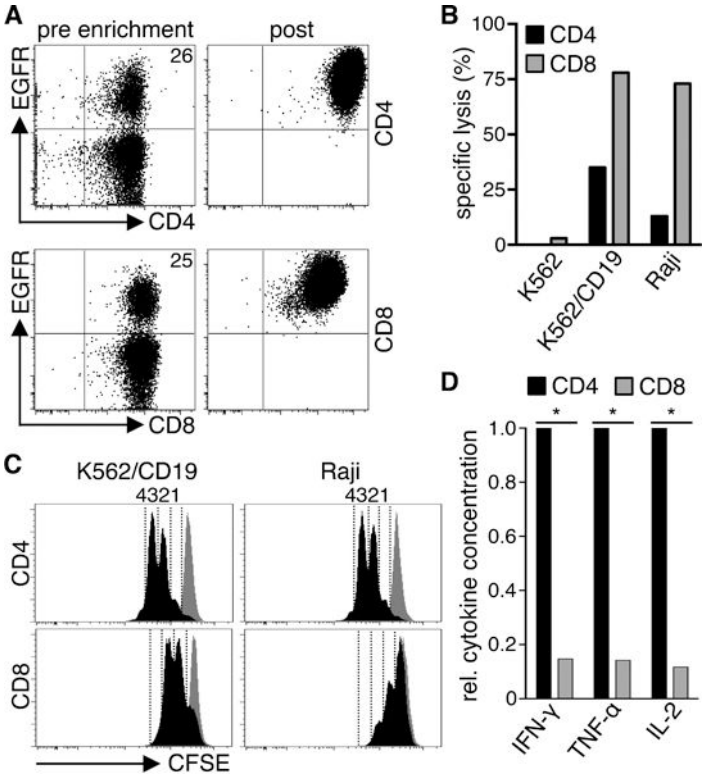

Figure 2. CD4$^+$ and CD8$^+$ CAR-T-cells differ in effector function

(A) Expression of EGFRt on CD4$^+$ and CD8$^+$ T-cells transduced with a CD19 CAR-EGFRt construct before enrichment (pre) and after enrichment and expansion (post). **(B)** Cytolytic activity of CD19 CAR-T-cells against ^{51}Cr-labeled CD19$^+$ (K562/CD19, Raji) and control (K562) target cells at an E:T ratio of 30:1 analyzed by a standard 4 h chromium release assay. **(C)** Proliferation of CFSE-labeled CD19 CAR-T-cells after stimulation with K562/CD19 and Raji cells for 72 h measured by CFSE dye dilution. Stimulation of CFSE-labeled CD19 CAR-T-cells with CD19$^-$ K562 cells is shown as a comparison in each histogram (gray graph). Numbers above each histogram indicate the number of cell divisions the proliferating subset underwent. Data in A–C are representative of experiments with CAR-T-cells derived from three different donors. **(D)** Relative cytokine production by CD19 CAR-T-cells after co-culture with K562/CD19 and Raji cells for 24 h. Data from three independent experiments with T-cells prepared from different donors were combined. Cytokine production of CD4$^+$ cells was set as 1 and relative cytokine production of CD8$^+$ T-cells was calculated. Asterisk indicates significant differences between CD4$^+$ and CD8$^+$ cells.

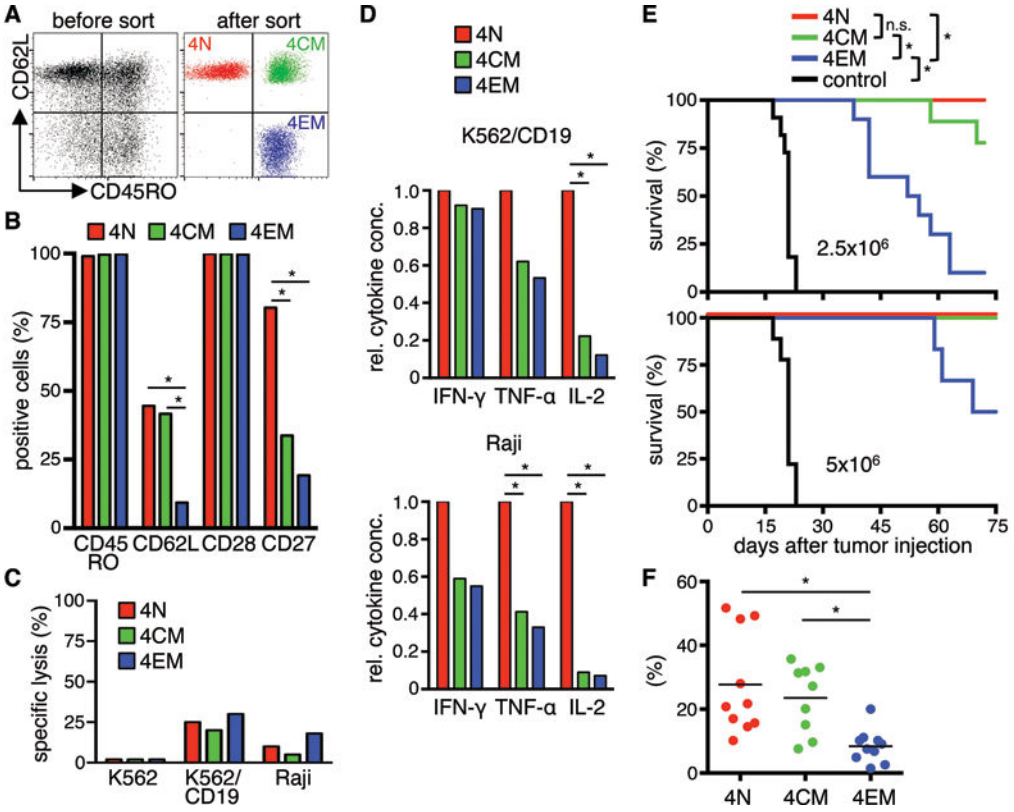

Figure 3. ***In vitro*** **and** ***in vivo*** **analysis of CD19 CAR-expressing naïve and memory CD4$^+$ T-cell subsets**

(A) CD4$^+$ T_N, T_{CM}, and T_{EM} cells were isolated by FACS. **(B)** Analysis of cell surface expression of CD45RO, CD62L, CD27, and CD28 on CD4$^+$ CD19 CAR-T-cells derived from different subsets. Data from three independent experiments with T-cells prepared from different donors were combined. **(C)** Cytolytic activity of CAR-T-cells against ^{51}Cr-labeled K562, K562/CD19, and Raji cells at an E:T ratio of 30:1 after 4 h. **(D)** Relative cytokine production by CD19 CAR-T-cells after co-culture with CD19$^+$ cells for 24 h. Data from three independent experiments with T-cells prepared from different donors were combined. Cytokine production of T_N was set as 1 and relative cytokine production of T_{CM} and T_{EM} was calculated. **(E)** Survival of Raji/ffluc-bearing NSG mice treated on day seven after tumor injection with CD19 CAR-T-cells derived from different CD4$^+$ T-cell subsets (2.5×10^6 or 5×10^6 CAR-T-cells per mouse). NSG mice that received 5×10^6 T-cells transduced with a vector encoding EGFRt alone (EGFRt-T-cells) were used as control. Asterisk indicates significant differences between groups (n.s.: not significant). Data from three independent experiments for the lower cell dose (2.5×10^6) and two for the higher cell dose (5×10^6) with minimum three mice per group were combined. **(F)** Frequency of transferred T-cells (human CD45$^+$/CD4$^+$) on day ten after T-cell transfer in peripheral blood of mice that had received the lower T-cell dose.

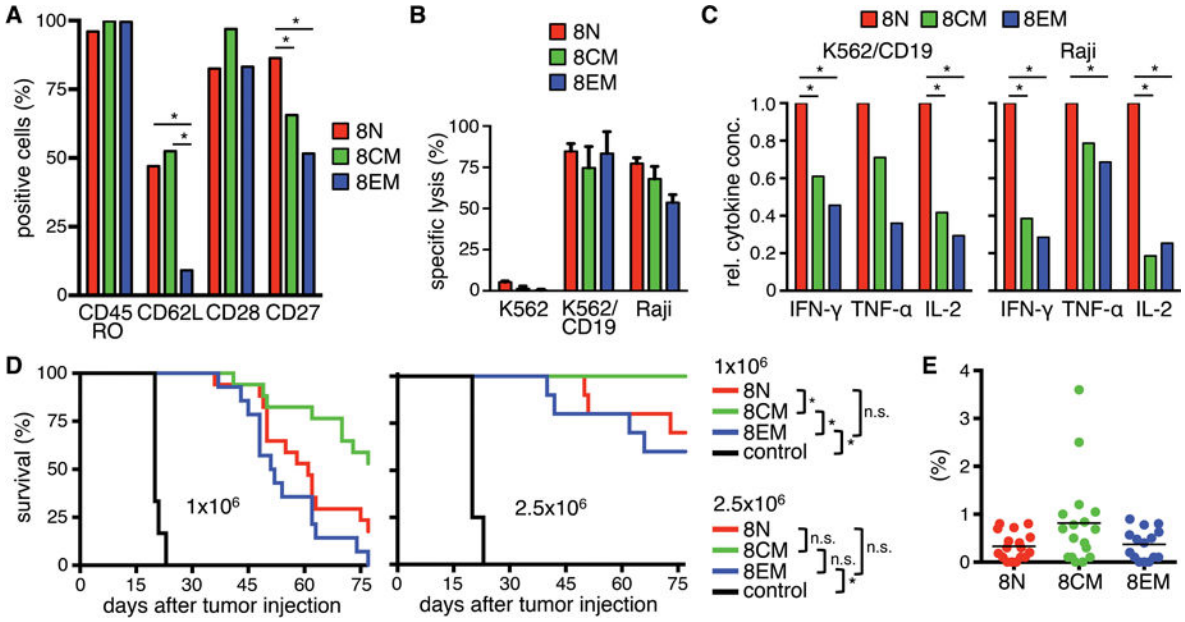

Figure 4. In vitro and in vivo analysis of CD19 CAR-expressing naïve and memory CD8$^+$ T-cell subsets

(A) Analysis of cell surface expression of CD45RO, CD62L, CD27, and CD28 on CD8$^+$ CD19 CAR-T-cells derived from naïve and memory subsets. Data from three independent experiments with T-cells prepared from different donors were combined. **(B)** Cytolytic activity of CD19 CAR-T-cells against ^{51}Cr-labeled K562, K562/CD19, and Raji cells at an E:T ratio of 30:1 after 4 h. **(C)** Relative cytokine production by CD19 CAR-T-cells after co-culture with CD19$^+$ cells for 24 h. Data from three independent experiments with T-cells prepared from different donors were combined. Cytokine production of T_N was set as 1 and relative cytokine production of T_{CM} and T_{EM} was calculated. **(D)** Survival of Raji/ffluc-bearing NSG mice treated on day seven after tumor injection with different doses of CD19 CAR-T-cells derived from different CD8$^+$ T-cell subsets (1×10^6 and 2.5×10^6). NSG mice that received 2.5×10^6 EGFRt-T-cells were used as control. Asterisk indicates significant differences between groups (n.s.: not significant). For the lower cell dose (1×10^6) four and for the higher cell dose (2.5×10^6) three experiments with minimum three mice per group are combined. **(E)** Frequency of transferred T-cells (human CD45$^+$/CD8$^+$) on day ten after T-cell transfer in peripheral blood of mice that had received the lower T-cell dose.

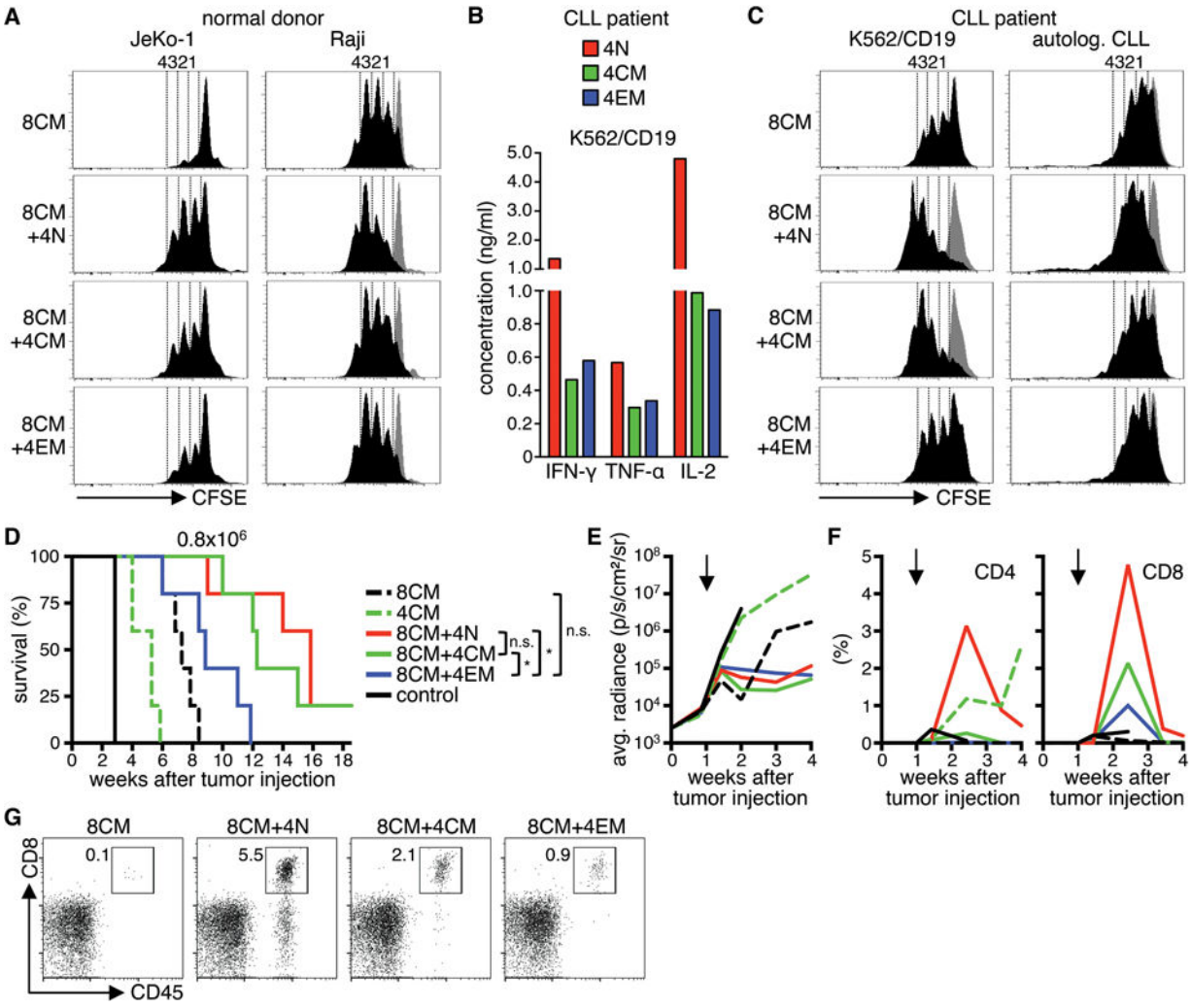

Figure 5. CD4$^+$ CD19 CAR-T-cells provide help to CD8$^+$ CD19 CAR-T-cells in vitro and in vivo

(A) Proliferation of CFSE-labeled CD8$^+$ T_{CM}-derived CD19 CAR-T-cells after stimulation with JeKo-1 and Raji cells for 72 h in the presence of CD4$^+$ CD19 CAR-T-cells derived from different subsets. Histograms are gated on CD8$^+$ T-cells. Stimulation with K562 cells is shown as a comparison in each histogram (gray graph). Data are representative for four independent experiments with T-cells generated from different healthy donors. **(B)** Cytokine production of CD4$^+$ CD19 CAR-T-cells derived from different subsets from a CLL-patient after co-culture with K562/CD19 for 24 h. **(C)** Same as **(A)** with T-cells from a CLL-patient and K562/CD19 cells and autologous CLL as stimulator cells in the assay. Data in **(B)** and **(C)** are representative for two independent experiments with T-cells generated from different patients. **(D)** Survival of Raji/ffluc-bearing NSG mice treated on day seven after tumor injection with 8×10^5 CD19 CAR-T-cells derived from CD4$^+$ T_N, T_{CM}, T_{EM}, and CD8$^+$ T_{CM} (CD4/CD8 combinations: 4×10^5 CD4$^+$ cells + 4×10^5 CD8$^+$ cells; 5 mice per group). NSG mice that received a combination of CD4$^+$ and CD8$^+$ EGFRt-T-cells were used as control. **(E)** Bioluminescence imaging of tumor growth. Arrows mark the day of T-cell transfer. **(F)** Frequency of transferred CD4$^+$ and CD8$^+$ T-cells (human CD45$^+$/CD4$^+$ or CD45$^+$/CD8$^+$) in

peripheral blood. **(G)** Flow cytometry data on day ten after T-cell transfer. Mice with median T-cell frequency are shown for each group.

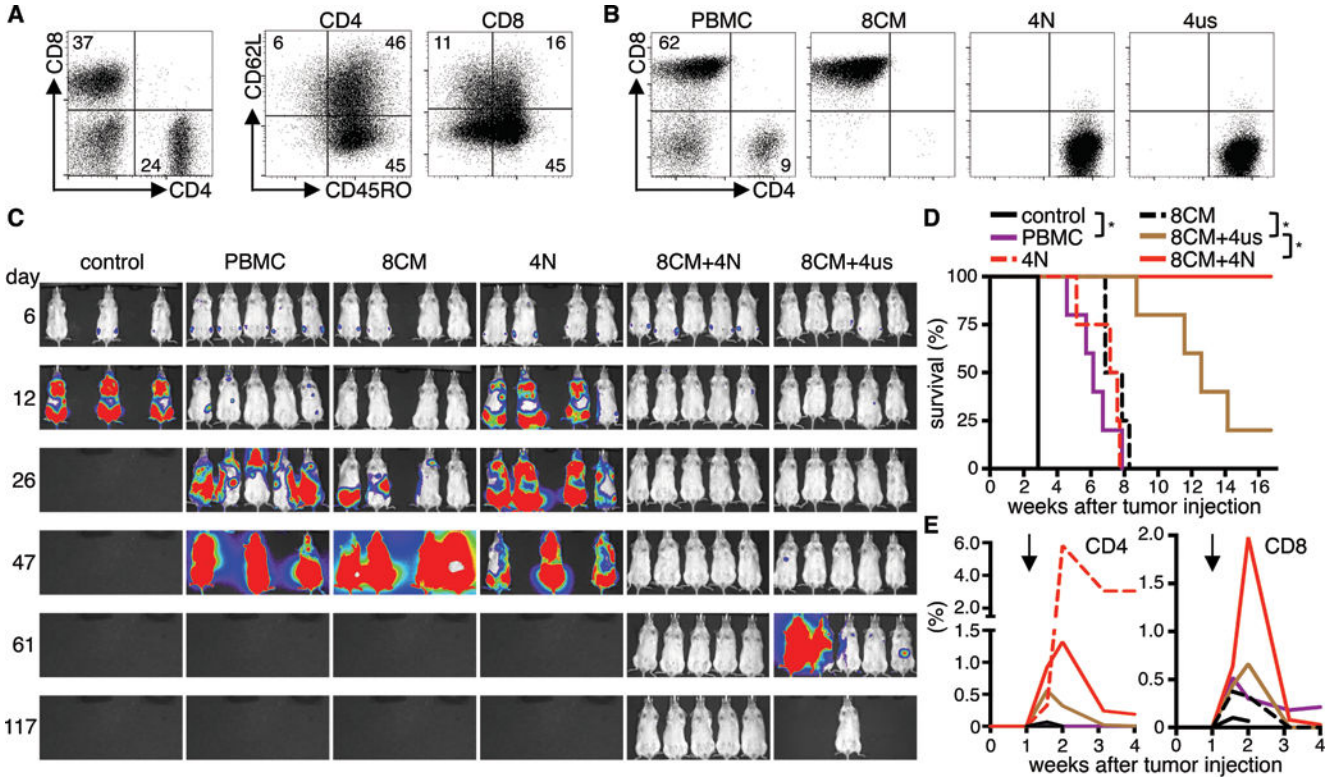

Figure 6. T-cell products of defined subset composition prepared from patients have enhanced potency

(A) T-cell subset composition in PBMC from a lymphoma patient. **(B)** CD4/CD8 phenotype of CD19 CAR-T-cell products derived from PBMC or from different sort-purified subsets. **(C)** Bioluminescence imaging data from Raji/ffluc-bearing NSG mice that had received 1×10^6 CD19 CAR-T-cells (CD4/CD8 ratio: 1:1, 4–5 mice per group). NSG mice that received EGFRt-T-cells were used as control (3 mice). **(D)** Survival and **(E)** persistence of transferred $CD4^+$ and $CD8^+$ T-cells in the blood of mice shown in **(C)**. Asterisk indicates significant differences between groups. Arrows mark the day of T-cell transfer. Data are representative for two independent experiments with T-cells generated from different patients.